Hair follicles are required for optimal growth during lateral skin expansion

Jack Heath[1,5], Abigail K. Langton[1,5], Nigel L. Hammond[1], Paul A. Overbeek[2], Michael J. Dixon[1,3] and Denis J. Headon[4]

[1]Faculty of Life Sciences, University of Manchester, Oxford Road, Manchester M13 9PT, UK
[2]Department of Molecular and Cellular Biology, Baylor College of Medicine, Houston, TX 77030, USA
[3]School of Dentistry, Faculty of Medical and Human Sciences, University of Manchester, Manchester, UK
[4]The Roslin Institute and Royal (Dick) School of Veterinary Studies, University of Edinburgh, Midlothian, EH25 9PS, UK
[5]Equal contribution

To whom correspondence should be addressed.
E-mail: denis.headon@roslin.ed.ac.uk

Keywords: Epidermis, stem cell, hair follicle, growth

Abbreviations: atRA, all-trans retinoic acid; Edar, Eda receptor; Edaradd, Edar-associated death domain; En, embryonic day n; HF, hair follicle; IFE, interfollicular epidermis; Pn, postnatal day n.

Short title: Hair follicles contribute to skin growth

The hair follicles and the interfollicular epidermis of intact mature skin are maintained by distinct stem cell populations. Upon wounding, however, emigration of hair follicle keratinocytes to the interfollicular epidermis plays a role in acute stages of healing. In addition to this repair function, rapidly cycling cells of the upper hair follicle have been observed transiting to the interfollicular epidermis in neonatal skin. Here we report that an absence of hair follicle development leads to shortening and kinking of the mouse tail. These skeletal defects are reduced by stimulating keratinocyte proliferation, suggesting that they arise from impaired epidermal expansion. We confirm that rapidly cycling cells of the hair follicle emigrate to the interfollicular epidermis of the neonatal tail. These results suggest that an absence of hair follicles results in impaired skin growth that is unable to keep pace with the rapidly elongating axial skeleton of the tail. Thus, in addition to their role in wound repair, hair follicles can make a significant contribution to lateral expansion of the interfollicular epidermis in the absence of trauma.

Introduction

The relationship between hair follicles and the non-follicle components of the skin has been studied for several decades. The cyclical growth and regression of hair follicles in the adult is associated with distinct alterations of skin structure, from the epidermis through to the deepest cutaneous tissues (Chase et al., 1953; Hansen et al., 1984; Paus et al., 1990), likely achieved primarily via a signalling interplay between hair follicles and other skin components (e.g. Plikus et al., 2008). In addition to these signal interactions, hair follicles are known to make a direct cellular contribution to the interfollicular epidermis (IFE) during wound repair (Bishop, 1945). Analyses of cell proliferation dynamics (Taylor et al., 2000) and recombinase-based lineage tracing (Ito et al., 2005; Levy et al., 2005) have enabled a careful tracing of hair follicle cells during epidermal homeostasis and repair. These methods agree that homeostasis of intact mature epidermis in the mouse does not involve emigration of cells from the hair follicles, but that wounding of the epidermis causes rapid and extensive migration of hair follicle keratinocytes to the IFE wound bed. In addition, however, a hair follicle contribution to the neonatal IFE has been suggested by Taylor and colleagues (Taylor et al., 2000), who took advantage of the relatively rapid cycling of cells in the upper hair follicle to label these cells and track their egress into the IFE. However, a neonatal keratinocyte provision was not detected by cre-based lineage analysis using the *Shh* promoter, which is expressed by cells of the embryonic hair follicle placode. The *Shh::cre* line produced labelled cells throughout almost the entire hair follicle, including the bulge and lower follicle, but some cells in the infundibulum of the upper follicle were noted to lack label, as did the entire IFE (Levy et al., 2005). Thus it is unclear whether hair follicles make a contribution to IFE expansion in the absence of injury.

Recombinase-based cell lineage tracing methods yield very reliable and reproducible data, but are limited by the availability of promoters specific to the cell type of interest. The cellular complexity of the hair follicle (Botchkarev and Paus, 2003) makes it difficult to identify a promoter that is active throughout the entire epithelial component of the follicle. Recently hair follicle progenitor cells more superficial than the bulge have been identified (Jensen et al., 2008; Nijhof et al., 2006) and it appears that the follicle contains a range of progenitor cell populations or behaviours, only some of which are targeted by currently defined promoters.

Here we have addressed the relationship between hair follicles and the IFE during neonatal skin expansion using the *Edaradd*$^{cr/cr}$ mutant mouse line. This mutant line carries a deletion of the entire *Edaradd* gene, which encodes a cytoplasmic signalling adapter that transduces signals from the cell surface receptor Edar (Headon et al., 2001). Transmission of the Edar signal is essential for normal development of a range of ectodermal appendages, including teeth, eccrine and Meibomian glands, and some hair follicles. In the absence of this signal hair follicles are produced on the trunk only from embryonic day 16 (E16), rather than E14 as in wild type, and no hair follicles are produced on the tail, which displays a characteristic kink (Thesleff and Mikkola, 2002). We find that cell emigration from hair follicles occurs in neonatal tail skin, that a lack of epidermal Edaradd function causes tail kinking, and that elevation of epidermal proliferation reduces tail kinking in the absence of hair follicle development. These data suggest that in the neonatal period hair follicle-derived cells provide a significant contribution to the IFE, aiding in skin expansion during a period of rapid body growth.

Results

A lack of hair follicles causes tail kinking and shortening

The *Edaradd*$^{cr/cr}$ mutant tail lacks hair follicles and exhibits distinctive zigzag kinks that gave this mutant allele its original name; crinkled. We examined the developmental time course of tail kinking by alcian blue staining of neonatal mutant tails to visualise the vertebral elements. Tail kinks are not present at birth, but by 2 days after birth *Edaradd* mutant mice develop undulations along the distal part of the tail, which resolve into a kink at the tip (Figure 1a). This skeletal malformation stands out as an unusual feature of the *Edaradd* mutant phenotype as the other affected structures are chiefly derived from the ectodermal cell lineage (Thesleff and Mikkola, 2002). The expression of components of the Edar signalling pathway in the cells surrounding condensing cartilage elements of the tail vertebrae (Figure 1b,c), initially suggested that the tail kinking defect in these mutants might be a direct consequence of aberrant bone development. However, in their original description of the crinkled mutant Falconer and colleagues suggested that the tail kinks are "simply a mechanical result of the sheath of the skin elongating more slowly than the skeleton which it surrounds" (Falconer et al., 1951). Such slow expansion of the skin would be consistent with the absence of a crucial input emanating from the hair follicles on the mutant tail. We tested Falconer's hypothesis by rescuing the crinkled mutant with an *Edaradd* cDNA transgene expressed specifically in the basal epidermis from the *Keratin14* promoter (Vassar et al., 1989). This transgene rescued hair follicle formation and also straightened the kinked tail of *Edaradd*$^{cr/cr}$ mutants (Figure 1d,e). In addition, we found that the tails of *Edaradd*$^{cr/cr}$ mutants are shorter than those of wild type mice and that the transgene rescues this tail length defect (Figure 1d,f). RT-PCR showed that the endogenous *Edaradd* gene is expressed in both neonatal tail skin and internal tissue, and, as expected, the *K14::Edaradd* transgene is expressed in the skin but not in developing skeletal elements (Fig. 1g). This experiment demonstrates

that a defect in the mutant epidermis is primarily responsible for tail shortening and kinking.

Morphology of the tail axial skeleton in the *Edaradd* mutant

We examined vertebral morphology and organisation by alcian blue and alizarin red staining of 5 week old wild type, *Edaradd*$^{cr/cr}$ mutant and *Edaradd*$^{cr/cr}$*,K14::Edaradd* rescued tails. The skeletal structure of wild type and rescued mutant tails were indistinguishable (Figure 2a,b), while the mutant tails showed misaligned vertebrae, one or more pronounced kinks, and impacted vertebrae present at the deflection points of the kinks (Figure 2c).

Tail shortening could be a consequence of a reduction in vertebral number, shortening of individual vertebrae, or reduction of the intervertebral spaces. We found that vertebral number is unchanged by the *Edaradd* mutation and that the length of the 25th caudal vertebra, near the tip of the tail, is also unchanged (Figure 2d). Thus, despite occasional incidences of impaction producing a malformed vertebra, the individual vertebrae of the kinked tails appear to be of normal length. The intervertebral spaces, however, are significantly reduced in the *Edaradd* mutant (Figure 2e). Overall, the primary effect of alopecic skin on the underlying skeleton is to cause closer packing of generally normal individual vertebrae.

Interfollicular epidermal proliferation is normal in the absence of hair follicles

That restoration of epidermal *Edaradd* expression in the crinkled mutant restores normal tail structure allows three general mechanisms to explain this rescue: i) that normal proliferation in the skin relies on hair follicle-derived signals or on an *Edaradd* function directly within the IFE, ii) that hair follicles directly influence developing skeletal elements to aid their alignment and spacing, or iii) that cells

migrate from the hair follicles to the skin and make a significant contribution to its lateral expansion.

We addressed the first of these possibilities by comparing the proliferative index of epidermal cells in neonatal *Edaradd*$^{cr/cr}$ mutant tail to the index in normal IFE (Figure 3a,b). We did not detect a difference in keratinocyte proliferation between genotypes, suggesting that neither hair follicle-derived signals, nor an IFE-autonomous Edaradd function, are required for normal neonatal IFE proliferation. This finding is somewhat surprising as epidermal thickness on the adult dorsum increases in early anagen, a phase of the hair cycle that closely resembles the morphogenesis of hair follicles in neonatal skin (Chase et al., 1953, Hansen et al., 1984).

To determine whether enhanced epidermal proliferation alone, in the absence of hair follicles and of *Edaradd* function, can rescue tail kinking, we topically treated newborn *Edaradd*$^{cr/cr}$ tail skin with all-trans retinoic acid (atRA) on postnatal days 0 and 2. atRA is a keratinocyte mitogen (Chapellier et al., 2002) and we found that topical treatment of neonatal tails with atRA significantly increases the proliferative index of *Edaradd*$^{cr/cr}$ basal keratinocytes (Figure 3a,c). We found that this treatment in the neonatal period also reduced the degree of kinking in the adult tail compared to untreated control animals (Figure 3d). That increasing the proliferation of mutant epidermis ameliorates tail kinking indicates that optimal epidermal growth during the neonatal period involves a hair follicle contribution to IFE expansion. In addition, since IFE proliferation in mutant skin is normal (Figure 3a,b) our results argue that follicles provide cells, rather than growth signals, to the IFE.

Hair follicles contribute cells to the neonatal interfollicular epidermis

To determine whether there is a direct cellular input from hair follicles to the IFE in the neonatal tail, we assessed whether keratinocyte emigration (Taylor et al., 2000) occurs on the tail. When administered to animals, the thymidine analogues chlorodeoxyuridine (CldU) and iododeoxyuridine (IdU) are incorporated into DNA by cells that are in S-phase. Each of these labels can be detected independently of the other in order to selectively tag and track cell populations with different proliferation dynamics (Figure 4a). Administration of CldU followed one hour later by IdU leads to double labelling of most proliferating cells (Figure 4b) as the duration of S-phase is greater than 1 hour. Administering CldU followed by IdU 24 hours later double labels cells in the hair follicles and in the IFE (Figure 4c), indicating cells that were in S-phase at the time of the CldU pulse and had reentered this phase 24 hours later. As reported for dorsal skin (Taylor et al., 2000), we found that the cell cycle for some hair follicle cells is shorter than that of keratinocytes in the IFE, since a 16 hour interval between CldU and IdU administration resulted in selective double labelling of cells in the hair follicles (Figure 4d,f). We followed the fate of these double labelled cells by chasing the IdU label for 24 hours prior to harvesting the tissue. This led to the appearance of double labelled cells in the IFE (Figure 4e,f), indicative of cell emigration from the follicles. The double labelled cells were found to be almost equally distributed between the hair follicles and the IFE, even though they were almost all located within the hair follicles when they were first labelled. Thus epidermal cells born in the hair follicles of the tail migrate to the IFE, as observed previously on the neonatal dorsum (Taylor et al., 2000) also occurs on the tail. Together, the data reported here suggest that these cells are required for optimal growth of the skin.

Discussion

Tail kinking is a relatively common phenotype displayed by mutant mouse lines (see Lyon et al., 1996). Where the cause of tail kinking has been studied, this phenotype is typically ascribed to defective development of internal tissues, such as the intervertebral disks (Semba et al., 2006), somites (Matsuura et al., 1998), neural tube (Franke et al., 2003) or found to be associated with bone defects that are manifest throughout the skeleton (Jena et al., 1997). In at least one case, that of the *Irf6* null mutant, defective cutaneous development has been shown to cause prenatal tail kinking due to fusion of the tail skin to the body wall (Richardson et al., 2006). The *Edaradd* mutant represents the first model in which skin growth has been linked to tail kinking.

That deficient epidermal growth due to a lack of hair follicles can cause tail kinking suggests that emigration of cells from the follicle makes an important functional contribution to IFE expansion, at least on the tail. However we are unable to exclude the possibility that hair follicles also make other contributions to skin growth. The highly integrated nature of hair follicles in the skin, and the potential interactions between the skin and growing musculo-skeletal system, allow for many possible follicle influences on tail kinking, from direct provision of dermal cells (Gharzi et al., 2003) to complex signalling interactions between follicles and deeper cutaneous structures (e.g. Plikus et al., 2008). However, our analysis of the cutaneous morphology of neonatal and adult tails (supplementary figure 1) did not identify gross structural defects in the *Edaradd*$^{cr/cr}$ mutant skin. The only difference identified was a thinning of the dermis of neonatal tail skin in the mutant. This thinning could be caused by a lack of growth factors emitted by downgrowing hair follicles to stimulate dermal thickening, as appears to occur in the anagen stage of the adult hair cycle (Chase et al., 1953; Hansen et al., 1984), a lack of a dermal cell provision from the

hair follicles (Gharzi et al., 2003) or to compression of the dermis between an expanding skeletal core and an abnormally taut epidermis.

While the presence of hair follicles on the trunk of adult *Edaradd*$^{cr/cr}$ animals limits our ability to study the generality of a relationship between absence of hair follicle development and tautness of skin, the delayed appearance of hair follicle primordia on the body provides an opportunity to address this question. We have noted when dissecting litters including *Edaradd*$^{cr/cr}$ and *Edaradd*$^{cr/+}$ embryos that the homozygous mutants are readily identifiable due to their translucent skin. Images of embryos show that E15 and E16 mutant skin appears to be tighter and less wrinkled than that of heterozygotes carrying hair placodes (supplementary figure 2). It remains to be determined, however, whether the skin of the neonatal trunk requires a hair follicle input for optimal lateral growth. It may be that the rapid increase in the tail's surface area necessitates a unique mechanism of skin growth.

The absence of skeletal defects in the *Edaradd*$^{cr/cr}$ tail until just after birth closely follows the previously reported loss of clonogenic keratinocytes from the mutant tail epidermis just before birth (Langton et al., 2008). Thus the clonogenic population, which resides largely in the hair follicles, is likely to play an important role in neonatal IFE expansion. However, these findings appear to contradict cell lineage studies in which tracing the progeny of the *Shh* expressing placode (Levy et al., 2005), or of the *Sox9* expressing cell population that ultimately produces the stem cells of the bulge (Nowak et al., 2008), found that a wound stimulus was required for the appearance of labelled cells in the IFE. A potential resolution of this apparent dichotomy is that not all cells of the mature hair follicle may be derived from *Shh* expressing precursors. The *Shh::cre* study found that the follicular infundibulum, located above the stem cell containing bulge region, contained some cells that were

not labelled (Levy et al., 2005). These upper follicle cells may be derived from the peripheral part of the embryonic hair placode, in which cells express placode markers such as *Dkk4* but do not express *Shh* (supplementary figure 3). In addition, cell lineage analyses performed by retroviral tagging suggest that in mature epidermis the upper follicle is a different compartment from the lower, and that the upper compartment can extend into the IFE (Ghazizadeh and Taichman, 2001). This upper follicle compartment contains an MTS24 expressing population that exists prior to formation of a definitive bulge (Nijhof et al., 2006), representing a good candidate population for a source of IFE cells during skin expansion.

Our work shows that hair follicles play a role in expansion of the neonatal tail skin, with the provision of keratinocytes to the IFE representing a likely, though perhaps not the only, mechanism for this effect. This supplementation of the IFE may occur not only in the neonatal period but at any time that the IFE's autonomous self-renewal mechanism (Clayton et al., 2007) fails to produce sufficient keratinocytes to maintain an intact, unstrained epidermis.

Materials and Methods

DNA synthesis labelling and detection

For double labelling with chlorodeoxyuridine (CldU) and iododeoxyuridine (IdU), P1 animals had 40 μg label/g body weight administered intraperitoneally. Skin samples were fixed in 4% paraformaldehyde, 6 μm paraffin sections were cut, antigen retrieval was performed in citrate buffer pH 6.0 and tissue sections were blocked using the M.O.M kit (Vector laboratories). IdU was detected using 1/100 mouse anti-BrdU (Becton Dickinson, Clone B44; recognises IdU and BrdU) followed by 1/100 goat

anti-mouse AlexaFluor 555 secondary antibody (Invitrogen). CldU was detected using 1/100 rat anti-BrdU (Abcam, BU1/75(ICR1); recognises CldU and BrdU) followed by 1/200 biotinylated goat anti-rat secondary antibody (Vector laboratories) and 1/100 streptavidin-Cy2 (Jackson ImmunoResearch, 1:100).
For determination of epidermal proliferative index, P2 *Edaradd*$^{cr/cr}$ and *Edaradd*$^{cr/+}$ littermates were intraperitoneally administered 20 μl/g body weight BrdU and FdU (Cell proliferation labeling reagent, GE Healthcare) and skin samples collected 2 hours later. Processed paraffin sections were incubated with rat anti-BrdU (Abcam) and DAB detection done using secondary antibody and Vectastain ABCperoxidase (Vector laboratories).

Skeletal staining

Tails were collected, skinned, fixed in 95% ethanol and stained in 150 mg/l alcian blue 8GX (Sigma-Aldrich) in 80% ethanol, 20% acetic acid. After staining samples were washed in 95% ethanol and cleared in 1% KOH. Bone was stained in 50 mg/l alizarin red (Sigma-Aldrich) in 1% KOH and samples were photographed after transfer to glycerol.

In situ hybridisation

A full length [35S]-labelled *Edar* antisense cRNA was hybridised to 10 μm paraffin wax embedded tissue sections as described (Headon and Overbeek, 1999).

Animals

Animals were maintained at 21°C. Experimental animals were obtained from *Edaradd*$^{cr/cr}$ x *Edaradd*$^{cr/+}$ crosses or from *Edaradd*$^{cr/cr}$ X *Edaradd*$^{cr/+}$,*K14::Edaradd* crosses. Transgenic *K14::HA-Edaradd* animals were generated by encoding two HA tags at the 5' end of the mouse *Edaradd* cDNA. This fusion sequence was cloned

downstream of a 2.27 kb human *Keratin14* promoter and generic intron, and a human growth hormone polyadenylation sequence was placed 3′ to the cDNA (Kucera et al., 1996). Linearised DNA was used for pronuclear injection. To stimulate epidermal proliferation in neonatal skin, tails were dipped in 0.5% all-trans retinoic acid (Sigma) dissolved in DMSO on days P0 and P2. All animal procedures were performed with institutional and UK Home Office approval.

Morphometric measurements

Digital images were collected and dimensions measured using ImagePro PLUS software package (MediaCybernetics). Tail length was measured along the centre of the tail and followed around the kink.

PCR

For RT-PCR, RNA was isolated using TRI Reagent (Sigma) and reverse transcribed using random primers and AMV RT (Roche) in a 20 μl reaction. Reactions were diluted 10 fold and 2 μl used as template.

For genotyping PCR, genomic DNA was prepared by placing ear clips in 300 μl 50 mM NaOH at 95°C for 20 minutes and 1 μl used as template. Thermal cycling conditions were: 5 min 95°C, 34 cycles of 30 s at 94°C, 30 s at 54°C and 1 min at 72°C. The sequences of the oligonucleotides used are given in the supplementary methods.

Conflict of interest

The authors state no conflict of interest

Acknowledgements

This work was supported by a grant from Giuliani SpA, Milan.

References

Bishop GH (1945) Regeneration after Experimental Removal of Skin in Man. *American Journal of Anatomy* 76:153-181.

Botchkarev VA, Paus R (2003) Molecular biology of hair morphogenesis: development and cycling. *Journal of experimental zoology Part B* 298:164-180.

Chapellier B, Mark M, Messaddeq N, Calleja C, Warot X, Brocard J, et al. (2002) Physiological and retinoid-induced proliferations of epidermis basal keratinocytes are differently controlled. *EMBO J* 21:3402-3413.

Chase HB, Montagna W, Malone JD (1953) Changes in the skin in relation to the hair growth cycle. *Anatomical Record* 116:75-81.

Clayton E, Doupe DP, Klein AM, Winton DJ, Simons BD, Jones PH (2007) A single type of progenitor cell maintains normal epidermis. *Nature* 446:185-189.

Falconer DS, Fraser AS, King JWB (1951) The genetics and development of crinkled, a new mutant in the house mouse. *Journal of genetics* 50:324-344.

Franke B, Klootwijk R, Hekking JW, de Boer RT, ten Donkelaar HJ, Mariman EC, et al. (2003) Analysis of the embryonic phenotype of Bent tail, a mouse model for Xlinked neural tube defects. *Anatomy and embryology* 207:255-262.

Gharzi A, Reynolds AJ, Jahoda CA (2003) Plasticity of hair follicle dermal cells in wound healing and induction. *Exp Dermatol* 12:126-136.

Ghazizadeh S, Taichman LB (2001) Multiple classes of stem cells in cutaneous epithelium: a lineage analysis of adult mouse skin. *EMBO J* 20:1215-1222.

Hansen LS, Coggle JE, Wells J, Charles MW (1984) The influence of the hair cycle on the thickness of mouse skin. *Anatomical Record* 210:569-573.

Headon DJ, Emmal SA, Ferguson BM, Tucker AS, Justice MJ, Sharpe PT, et al. (2001) Gene defect in ectodermal dysplasia implicates a death domain adapter in development. *Nature* 414:913-916.

Headon DJ, Overbeek PA (1999) Involvement of a novel Tnf receptor homologue in hair follicle induction. *Nat Genet* 22:370-374.

Ito M, Liu Y, Yang Z, Nguyen J, Liang F, Morris RJ, et al. (2005) Stem cells in the hair follicle bulge contribute to wound repair but not to homeostasis of the epidermis. *Nat Med* 11:1351-1354.

Jena N, Martin-Seisdedos C, McCue P, Croce CM (1997) BMP7 null mutation in mice: developmental defects in skeleton, kidney, and eye. *Experimental Cell Research* 230:28-37.

Jensen UB, Yan X, Triel C, Woo SH, Christensen R, Owens DM (2008) A distinct population of clonogenic and multipotent murine follicular keratinocytes residing in the upper isthmus. *Journal of Cell Science* 121:609-617.

Kucera GT, Bortner DM, Rosenberg MP (1996) Overexpression of an Agouti cDNA in the skin of transgenic mice recapitulates dominant coat color phenotypes of spontaneous mutants. *Developmental Biology* 173:162-173.

Langton AK, Herrick SE, Headon DJ (2008) An extended epidermal response heals cutaneous wounds in the absence of a hair follicle stem cell contribution. *J Invest Dermatol* 128:1311-1318.

Levy V, Lindon C, Harfe BD, Morgan BA (2005) Distinct stem cell populations regenerate the follicle and interfollicular epidermis. *Developmental Cell* 9:855-861.

Lyon, MF, Rastan S, Brown SDM. (1996) *Genetic Variants and Strains of the Laboratory Mouse*. Oxford University Press: Oxford

Matsuura T, Narama I, Ozaki K, Nishimura M, Imagawa T, Kitagawa H, et al. (1998) Developmental study on reduction and kinks of the tail in a new mutant knotty-tail mouse. *Anatomy and embryology* 198:91-99.

Nijhof JG, Braun KM, Giangreco A, van Pelt C, Kawamoto H, Boyd RL, et al. (2006) The cell-surface marker MTS24 identifies a novel population of follicular keratinocytes with characteristics of progenitor cells. *Development (Cambridge, England)* 133:3027-3037.

Nowak JA, Polak L, Pasolli HA, Fuchs E (2008) Hair follicle stem cells are specified and function in early skin morphogenesis. *Cell Stem Cell* 3:33-43.

Paus R, Stenn KS, Link RE (1990) Telogen skin contains an inhibitor of hair growth. *British Journal of Dermatology* 122: 777-784.

Plikus MV, Mayer JA, de la Cruz D, Baker RE, Maini PK, Maxson R, Chuong CM. (2008) Cyclic dermal BMP signalling regulates stem cell activation during hair regeneration. *Nature* 451:340-344.

Richardson RJ, Dixon J, Malhotra S, Hardman MJ, Knowles L, Boot-Handford RP, et al. (2006) Irf6 is a key determinant of the keratinocyte proliferation-differentiation switch. *Nature Genet* 38:1329-1334.

Semba K, Araki K, Li Z, Matsumoto K, Suzuki M, Nakagata N, et al. (2006) A novel murine gene, Sickle tail, linked to the Danforth's short tail locus, is required for normal development of the intervertebral disc. *Genetics* 172:445-456.

Taylor G, Lehrer MS, Jensen PJ, Sun TT, Lavker RM (2000) Involvement of follicular stem cells in forming not only the follicle but also the epidermis. *Cell* 102:451-461.

Thesleff I, Mikkola ML (2002) Death receptor signaling giving life to ectodermal organs. *Sci STKE* 2002:PE22.

Vassar R, Rosenberg M, Ross S, Tyner A, Fuchs E (1989) Tissue-specific and differentiation-specific expression of a human K14 keratin gene in transgenic mice. *Proceedings of the National Academy of Sciences of the United States of America* 86:1563-1567.

Figure Legends

Figure 1. An absence of hair follicles is the primary cause of tail kinking in the *Edaradd*$^{cr/cr}$ mutant. (**a**) Developmental time course of tail kinking in *Edaradd*$^{cr/cr}$ tails, illustrated by alcian blue staining of vertebral elements. The kink is not present at birth, but undulations appear along the tail length by P2 and are resolving into kinks at P3. Proximal is uppermost, distal at the bottom of the panel. Scale bar, 2 mm. (**b,c**) In situ hybridisation detects expression of *Edar* (white silver grains in c) in the epidermis and also between the cartilaginous condensations of the developing vertebral column. (**b**) Haemotoxylin stained bright field and (**c**) dark field images of E15 tail sections. (**d**) A *Keratin14::Edaradd* transgene (Tg) rescues hair follicle development and tail kinking in *Edaradd*$^{cr/cr}$ animals. Upper panel, gross view of P35 animals as labelled; lower panel, higher magnification of tail tips. (**e**) Genotyping of animals in (d) to detect the endogenous *Edaradd*, the *K14::Edaradd* transgene and *Actin* positive control. (**f**) Tail:body length ratios for P35 mice. *Edaradd*$^{cr/cr}$ mutants have shorter tails than wild type. Normal tail length is restored by the *K14::Edaradd* transgene. *** $p<0.001$. Error bars show S.E.M. (**g**) RT-PCR determination of endogenous and transgenic *Edaradd* expression. P1 tails were separated into 2 fractions: (i) skin and (ii) internal tissues, including the vertebral column. Endogenous *Edaradd* is expressed in both skin and internal tail tissue in wild type animals, while expression of the transgene is restricted to the skin fraction. WT = wild type; Tg = *K14::Edaradd* transgenic; cr = *Edaradd*$^{cr/cr}$.

Figure 2. Impaction of vertebrae and reduced intervertebral spacing in the mature *Edaradd*$^{cr/cr}$ tail. (**a-c**) Alcian blue and alizarin red staining of P35 tails from (**a**) wild type, (**b**) *Edaradd*$^{cr/cr}$, *K14::Edaradd* and (**c**) *Edaradd*$^{cr/cr}$ animals. Inset in (c) shows impacted vertebra at the tail kink. (**d**) Length of the 25th caudal vertebra,

which lies distal to the tail kink, of P35 mice. (**e**) Distance between the 17th and 18th caudal vertebrae, which lie proximal to the kink. A representative view of this intervertebral space for each genotype is shown above each data bar. ***p<0.001. Error bars show S.E.M. WT = wild type; cr,Tg = *Edaradd*$^{cr/cr}$,*K14::Edaradd*; cr = *Edaradd*$^{cr/cr}$

Figure 3. Increased epidermal proliferation reduces tail kinking caused by the absence of hair follicles. (**a-c**) Cell proliferation in P2 tail determined by BrdU incorporation. (**a**) Immunostained cross sections of P2 tails from animals administered BrdU, with or without topical all-trans retinoic acid (atRA) treatment. Hair follicles are apparent in *Edaradd*$^{cr/+}$ skin. (**b**) Quantification of IFE BrdU incorporation in P2 *Edaradd*$^{cr/+}$ (cr/+) and *Edaradd*$^{cr/cr}$ (cr/cr) tails. No significant difference between heterozygote IFE and homozygote mutant epidermis was detected. (**c**) Quantification of BrdU incorporation by P2*Edaradd*$^{cr/cr}$ epidermis with or without topical atRA treatment. Error bars show S.E.M. (**d**) Topical application of atRA to mutant tail skin in the postnatal period reduces the extent of kinking in the adult tail.

Figure 4. Emigration of hair follicle cells to the IFE in neonatal epidermis. (**a**) Schematic of cell labelling and tracking experiments. Administration of CldU to P2 animals and time points for IdU administration and tissue collection are indicated on a timeline. The circled letters indicate the panels below that show data for that treatment. (**b**) Administration of a pulse of CldU, followed at 1 hour by IdU and tissue collection 1 hour later yields chiefly double labelled cells (blue arrowheads) that appear yellow. The asterisks indicate erythrocyte autofluorescence. This shows that double labelled cells can be detected using this method. (**c**) A 24 hour interval between CldU and IdU pulses double labels cells of both the IFE and the hair follicles. Most cells are single labelled, demonstrating that single labelled cells can be

distinguished from double labelled ones. (**d**) A 16 hour interval between CldU and IdU pulses selectively double labels cells of the hair follicle. (**e**) A 16 hour interval between CldU and IdU pulses followed by a 24 hour chase period prior to tissue collection detects double labelled keratinocytes that have emigrated from the hair follicles to the IFE (blue arrowheads). The dotted line indicates the epidermal-dermal junction. Scale bar, 100 μm. (**f**) Quantification of the frequency of CldU, IdU double labelled cells in hair follicles and IFE pulsed with CldU and, 16 hours later, IdU. Skin samples were collected either 1 or 24 hours after IdU administration. The frequency of double labelled cells in the IFE is far greater at 24 hours post-IdU than at 1 hour, indicating emigration of double labelled cells from the hair follicles. Error bars show S.E.M.

Figure 1

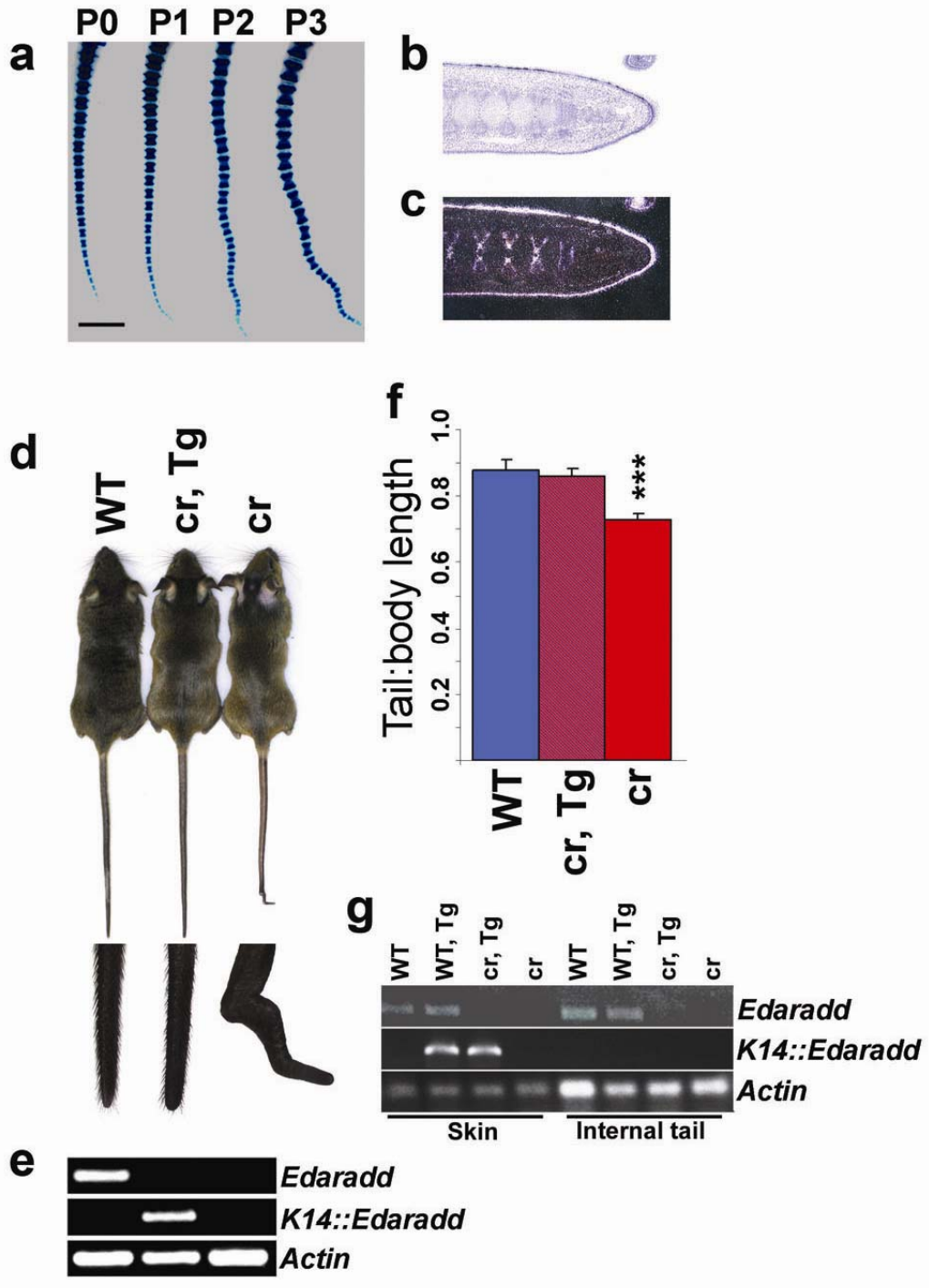
a
P0
P1
P2
P3
b
c
d
WT
cr, Tg
cr
f
Tail:body length
1.0
0.8
0.6
0.4
0.2
***
WT
cr, Tg
cr
g
WT
WT, Tg
cr, Tg
cr
WT
WT, Tg
cr, Tg
cr
Edaradd
K14::Edaradd
Actin
Skin
Internal tail
e
Edaradd
K14::Edaradd
Actin

Figure 2

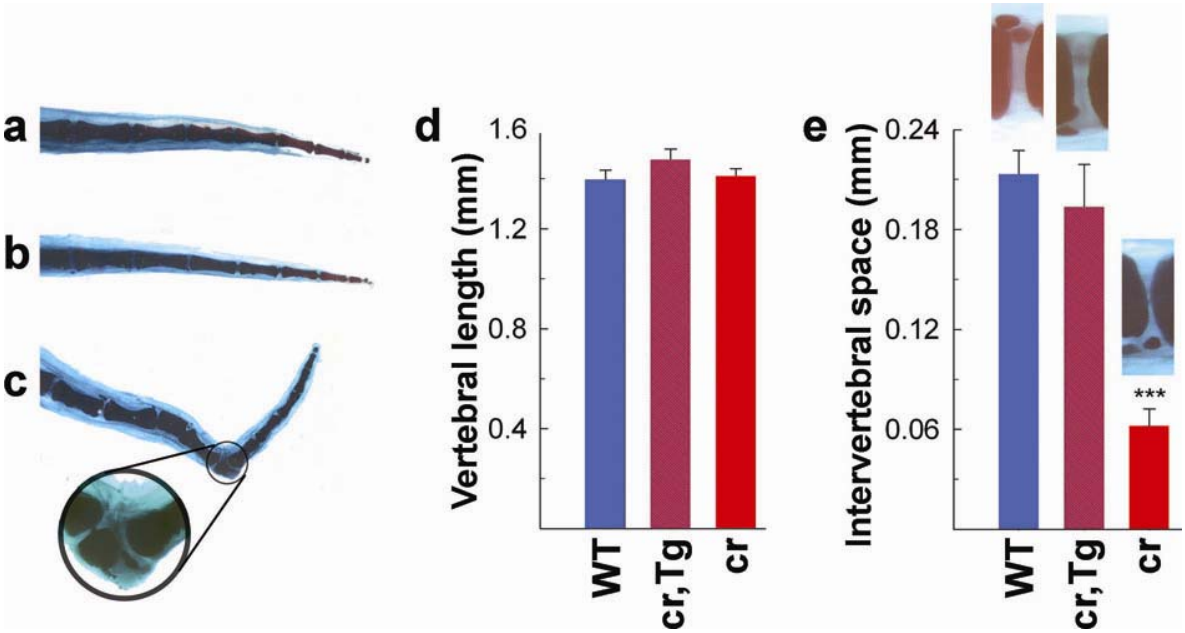
a
b
c
d
Vertebral length (mm)
1.6
1.2
0.8
0.4
WT
cr,Tg
cr
e
Intervertebral space (mm)
0.24
0.18
0.12
0.06
***
WT
cr,Tg
cr

Figure 3

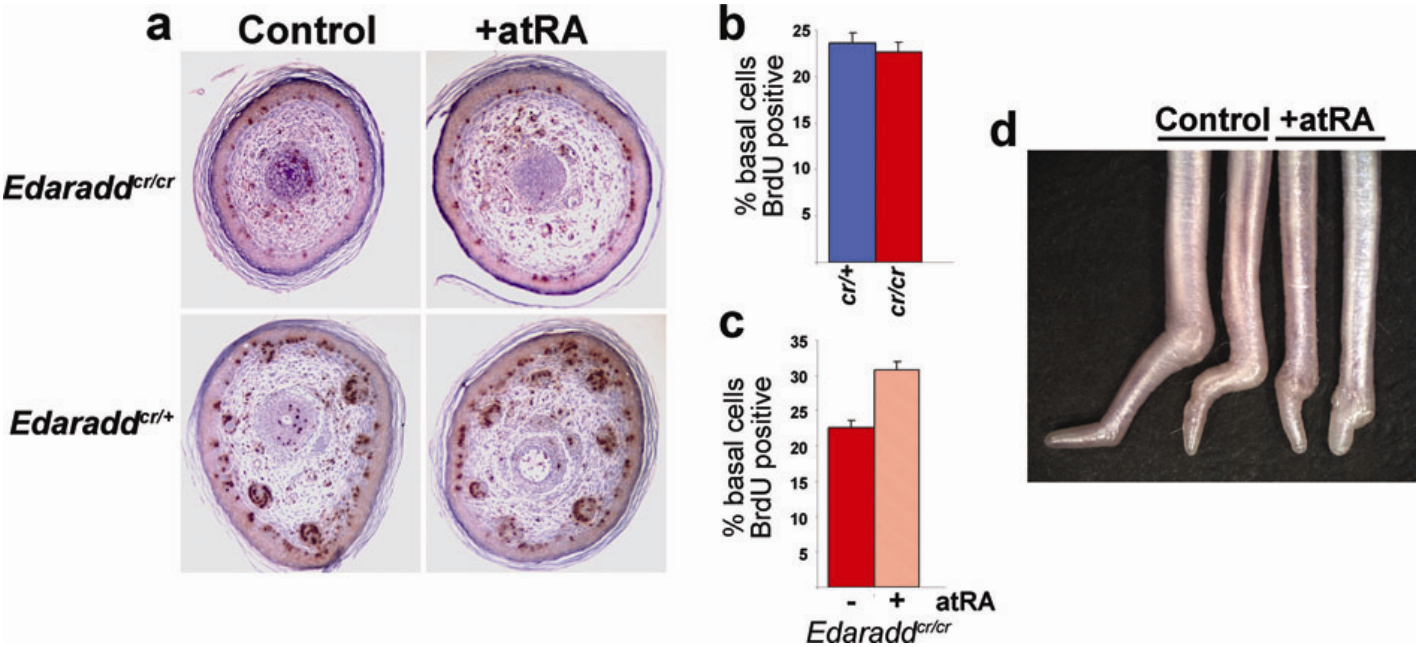
a
Control
+atRA
Edaradd cr/cr
Edaradd cr/+
b
% basal cells BrdU positive
25
20
15
10
5
cr/+
cr/cr
c
% basal cells BrdU positive
35
30
25
20
15
10
5
-
+
atRA
Edaradd cr/cr
d
Control
+atRA

Figure 4

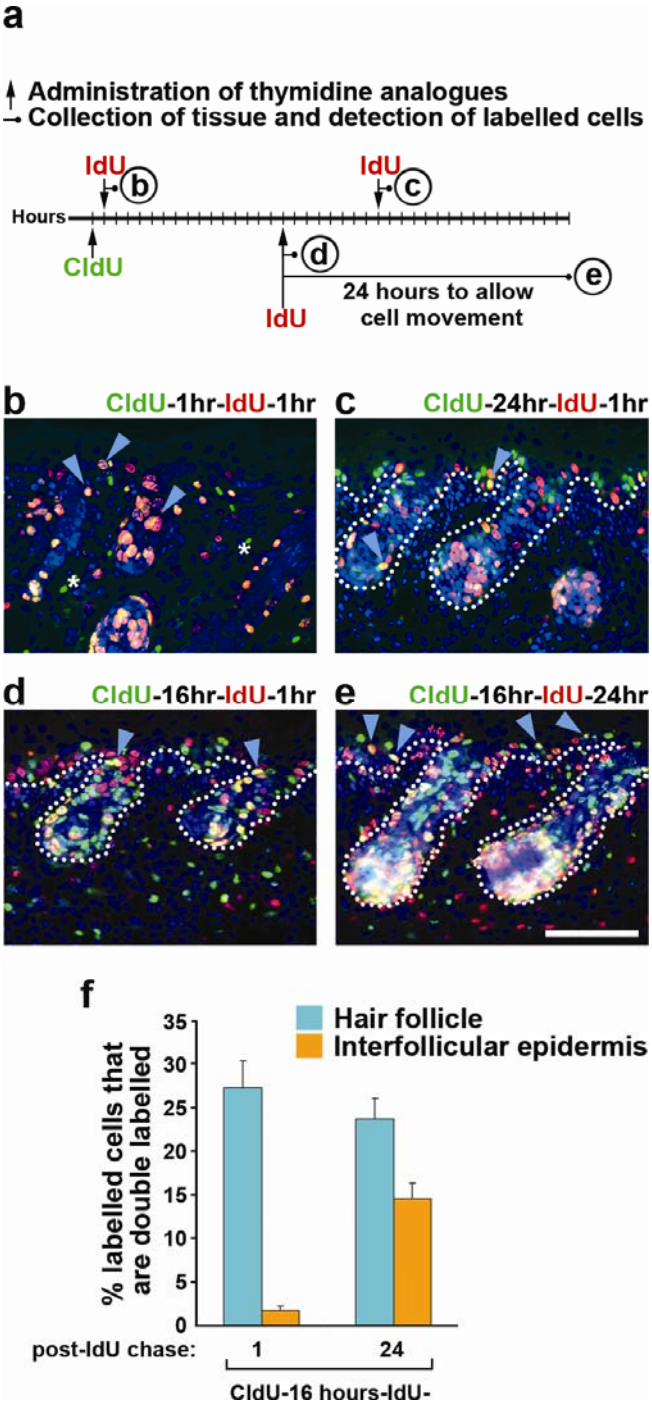
a
Administration of thymidine analogues
Collection of tissue and detection of labelled cells
IdU
b
IdU
c
Hours
CldU
d
e
24 hours to allow
cell movement
IdU
b
CldU-1hr-IdU-1hr
c
CldU-24hr-IdU-1hr
d
CldU-16hr-IdU-1hr
e
CldU-16hr-IdU-24hr
f
Hair follicle
Interfollicular epidermis
% labelled cells that
are double labelled
35
30
25
20
15
10
5
0
post-IdU chase:
1
24
CldU-16 hours-IdU-

Supplementary information

Hair follicles are required for optimal growth during lateral skin expansion

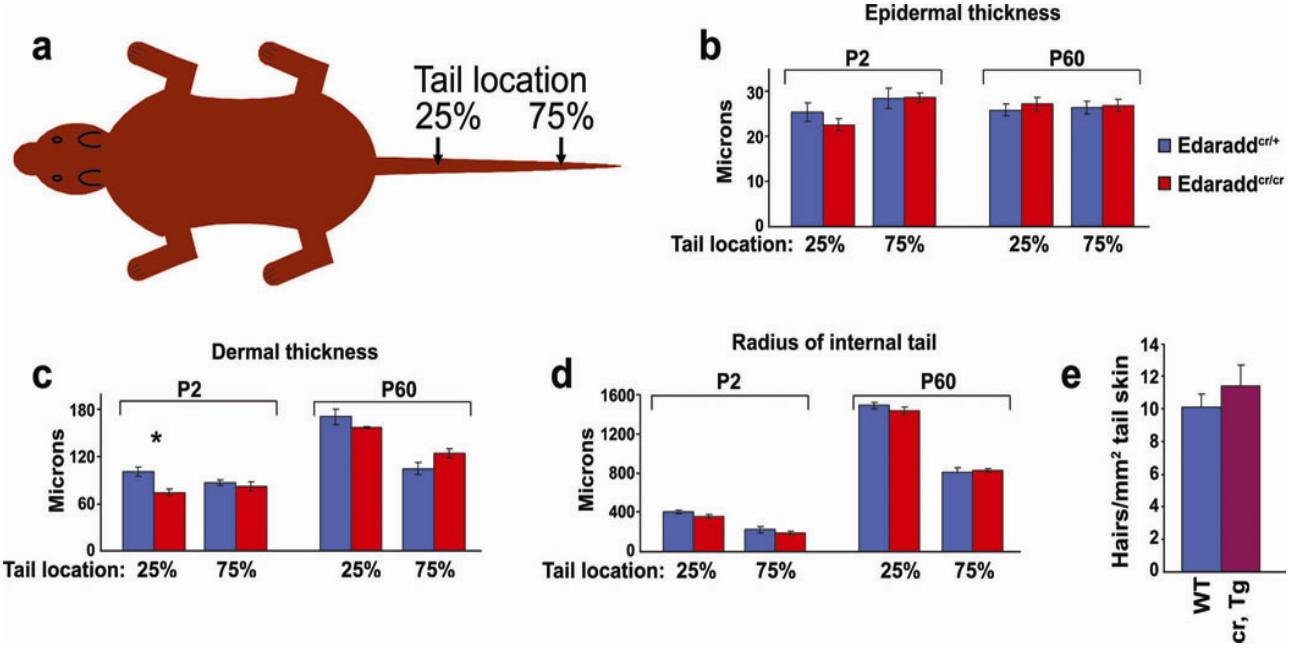

Figure S1. Morphometric analysis of tail skin with and without hair follicles. (**a**) Schematic of a mouse showing the locations at which tail samples were collected. *Edaradd*$^{cr/+}$ and *Edaradd*$^{cr/cr}$ tail skin was collected at proximal (25% tail length) and distal (**75%** tail length) sites from littermates at P2 and P60. All animals at P60 were male. (**b**) Epidermal thickness (not including the cornified layer), (**c**) dermal thickness and (**d**) the radius of the internal tail tissue (i.e. not including epidermis or dermis) were determined by measuring the area of each layer on transverse sections stained with haematoxylin and eosin. The only statistically significant difference detected between genotypes was dermal thickness at 25% tail length at P2, indicated by * ($p = 0.021$). (**e**) A normal tail hair density is restored by transgenic rescue of the *Edaradd*$^{cr/cr}$ mutation. The number of hairs per mm^2 at the mid-point of the tail was determined on 2 month old wild type (WT) and rescued *Edaradd*$^{cr/cr}$*,K14::Edaradd* transgenic (cr, Tg) animals. Error bars show S.E.M.

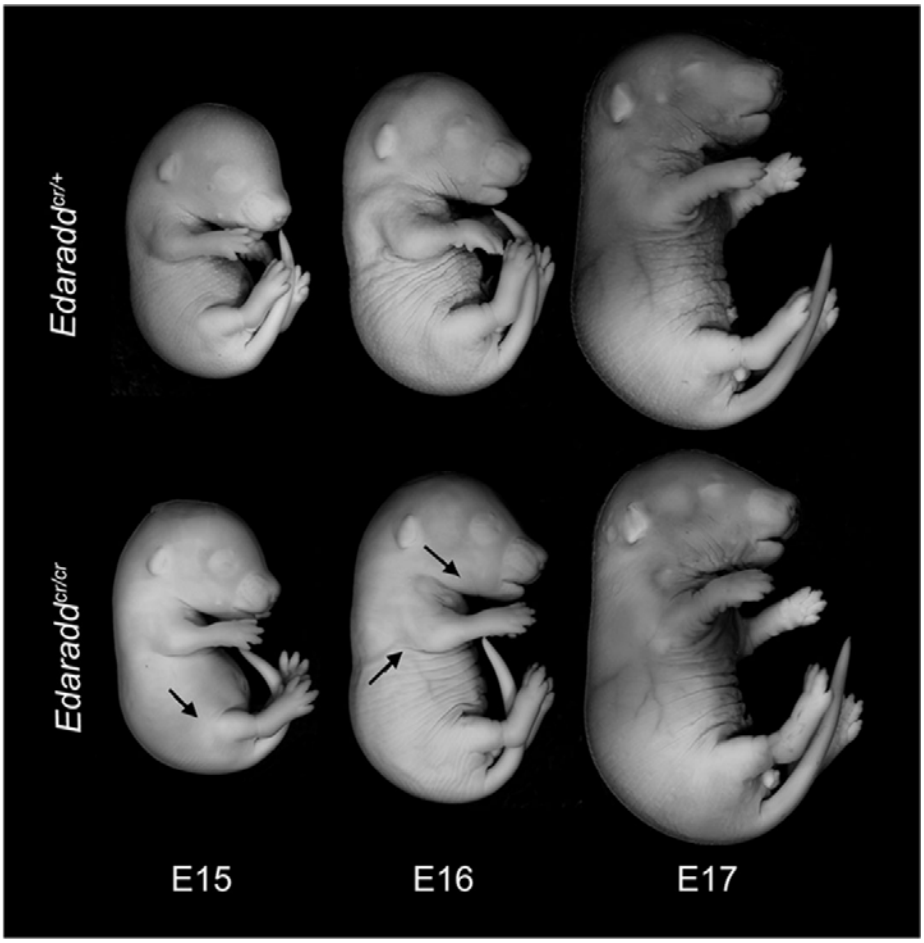

Figure S2. An absence of hair follicle placodes on the trunk leads to a reduction in skin wrinkling. Gross views of E15, E16 and E17 *Edaradd*$^{cr/+}$ and *Edaradd*$^{cr/cr}$ embryos. The heterozygous embryos produce hair follicle placodes from E14, but the homozygous mutants do not produce placodes until E16. *Edaradd*$^{cr/cr}$ skin appears to be smoother than that of *Edaradd*$^{cr/+}$ embryos at E15 and E16. Arrows indicate skin folds present in *Edaradd*$^{cr/+}$ but absent in *Edaradd*$^{cr/cr}$. Embryos at each age are littermates.

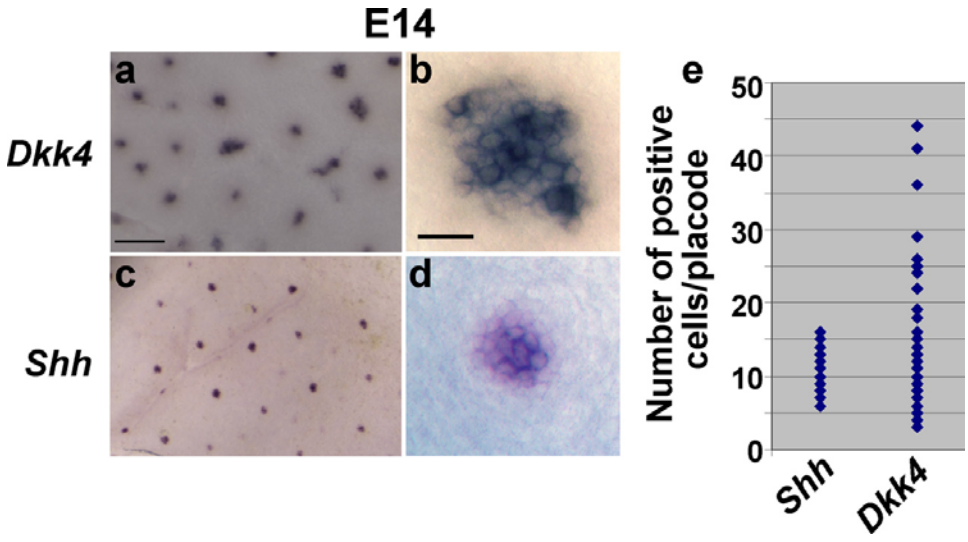

Figure S3. *Shh* is expressed in a more restricted placode domain than *Dkk4*. Whole mount in situ hybridisation detecting (**a,b**) *Dkk4* and (**c,d**) *Shh* in E14 wild type dorsolateral mouse skin. *Dkk4* is expressed in the placode in a broader and less regular domain than that of *Shh*. Scale bar for (**a,c**) 200 μm, for (**b,d**) 25 μm. (**e**) Scatterplot of the number of *Shh* and *Dkk4* expressing cells per placode in E14 skin. Cell number per placode was determined by counting the unstained nuclei surrounded by BCIP/NBT alkaline phosphatase reaction product.

Supplementary methods

Determination of IdU persistence in vivo

A long lived pool of IdU would confound interpretation of our pulse-chase cell tracking experiments. To confirm that IdU uptake did not occur beyond one hour after administration, we treated P2 wild type pups with IdU and collected skin samples 1,2, 4 or 20 hours later. We found that long chase periods did not increase the fraction of labelled basal epidermal cells beyond that labelled at 1 hour.

% IdU positive basal IFE cells on the tail

Collected post-IdU	1hour	2 hours	4 hours	20 hours
Animal 1	27.0	26.9	31.2	31.3
Animal 2	32.5	32.1	29.7	33.8

Oligonucleotide sequences used for PCR and RT-PCR

Actin positive control: forward 5'-GCTTCTGAGATGTCTCTCTCT-3'; reverse 5'-ACACAGGCTTTTGTAGGTTGC-3'

Endogenous *Edaradd* genomic DNA: forward 5'-GTCCACTTTAGCCGGATCTG-3'; reverse 5'-GTTCTTCACGGTTGGGTGAC-3'

Endogenous *Edaradd* cDNA: forward 5'-GTCCTCTCCTGGTCTTCATG-3'; reverse 5'-GTCCTCTGGCTGTTTCGGAA-3'

K14::Edaradd transgene gDNA: forward 5'-AGAGAATTCAGATCTATGGCT-3'; reverse 5'-TCTCCCTGAGGTTGGTCATC-3'

K14::Edaradd transgene cDNA: forward 5'-GCTTCTAGAATTCGCTGTCTG-3'; reverse 5'-TCTCCCTGAGGTTGGTCATC-3'